

# Single-Crystal $^{31}\text{P}$ NMR and X-ray Diffraction Study of a Molybdenum Phosphine Complex: (5-Methyldibenzophosphole)pentacarbonylmolybdenum(0)

Klaus Eichele,<sup>†</sup> Roderick E. Wasylishen,<sup>\*‡</sup> Kalyani Maitra,<sup>‡</sup> John H. Nelson,<sup>\*‡</sup> and James F. Britten<sup>§</sup>

Departments of Chemistry, Dalhousie University, Halifax, Nova Scotia, Canada B3H 4J3, University of Nevada, Reno, Nevada 89557-0020, and McMaster University, Hamilton, Ontario, Canada L8S 4M1

Received March 4, 1997<sup>⊗</sup>

The molecular structure of (5-methyldibenzophosphole)pentacarbonylmolybdenum(0), **1**, has been determined by X-ray crystallography. The crystal is monoclinic  $C2/c$ ,  $Z = 8$ , with unit cell dimensions of:  $a = 31.113(2)$  Å,  $b = 7.7917(5)$  Å,  $c = 17.9522(12)$  Å, and  $\beta = 122.135(4)^\circ$ . Least-squares refinement converged to  $R(F) = 0.0245$  for 2407 independent reflections. The molecular structure is typical of phosphine-substituted metal carbonyls. It contains an approximate mirror plane which bisects the dibenzophosphole framework. Phosphorus-31 NMR spectra of powder and single-crystal samples of **1** have been obtained with cross-polarization and  $^1\text{H}$  high-power decoupling. The  $^{31}\text{P}$  CP/MAS NMR spectra exhibit exceptionally well-resolved satellites due to spin–spin coupling interactions with  $^{95,97}\text{Mo}$  ( $I = 5/2$ ). Using first-order perturbation theory, the multiplets have been analyzed to yield  $^1J(^{95,97}\text{Mo}, ^{31}\text{P}) = 123(2)$  Hz and estimates of the molybdenum nuclear quadrupolar coupling constants,  $\chi(^{95}\text{Mo}) = -0.87$  MHz and  $\chi(^{97}\text{Mo}) = 10.1$  MHz. Phosphorus-31 NMR spectra of a large single crystal of **1** have been investigated as a function of orientation about three orthogonal axes in the applied magnetic field. Analysis of the data yields the three principal components of the phosphorus chemical shift tensor,  $\delta_{11} = 112$  ppm,  $\delta_{22} = -23$  ppm, and  $\delta_{33} = -40$  ppm;  $\delta_{22}$  lies close to the Mo–P bond ( $8^\circ$ ), while  $\delta_{11}$  lies in the approximate mirror plane. The phosphorus chemical shift tensor determined for **1** is compared with the limited anisotropic phosphorus shift data available in the literature.

## Introduction

Recently, we reported the results of a  $^{31}\text{P}$  nuclear magnetic resonance (NMR) study of a series of group 6 transition metal complexes containing 5-phenyldibenzophosphole (PhDBP) of the types  $(\text{PhDBP})\text{M}(\text{CO})_5$  and  $\text{cis}-(\text{PhDBP})_2\text{M}(\text{CO})_4$ , where  $\text{M} = \text{Cr}, \text{Mo},$  or  $\text{W}$ .<sup>1</sup> Analysis of the spectra obtained by examining stationary powder samples indicated that the principal component of the chemical shift tensor corresponding to the direction of greatest phosphorus shielding,  $\delta_{33}$ , is relatively insensitive to the metal. In contrast, the other two principal components of the phosphorus chemical shift tensor,  $\delta_{11}$  and  $\delta_{22}$ , show considerable variation but decrease systematically on descending the group from Cr to W. These observations were rationalized in terms of variations in the paramagnetic contribution to the phosphorus shielding. The importance of this term is related to how well the orbital angular momentum operators mix occupied and virtual orbitals perpendicular to the direction of the applied magnetic field.<sup>2</sup> Therefore, a change of the M–P bond should be most clearly expressed in the phosphorus chemical shift components perpendicular to the M–P bond, while the direction along the M–P bond should be less sensitive. According to this model, the most shielded direction in the PhDBP complexes was assigned to the direction of the M–P bond. Similar conclusions have been reached for chelate

complexes involving molybdenum and tungsten,<sup>3,4</sup> and recent density functional theory calculations of  $^{31}\text{P}$  shieldings in complexes of type  $\text{LM}(\text{CO})_5$  ( $\text{L} = \text{PH}_3, \text{PMe}_3, \text{PF}_3, \text{PCl}_3$ ;  $\text{M} = \text{Cr}, \text{Mo}, \text{W}$ ) seem to confirm this notion.<sup>5</sup> However, besides these qualitative arguments supported by recent theoretical calculations, no firm experimental data on the orientation of  $^{31}\text{P}$  chemical shift tensors in the molecular frame are available for phosphine complexes of group 6 transition metals, and little is known about other transition metal complexes. In general, NMR studies of powder samples do not provide information concerning the orientation of shielding tensors. So far, the orientation of phosphorus shielding tensors of only two mercury phosphines<sup>6,7</sup> and one rhodium phosphine complex<sup>8</sup> have been characterized via  $^{31}\text{P}$  single-crystal NMR. Here, we present the results of a single-crystal  $^{31}\text{P}$  NMR investigation of (5-methyldibenzophosphole)pentacarbonylmolybdenum(0),  $(\text{OC})_5\text{Mo}(\text{MeDBP})$ , **1**.

## Experimental Section

**Sample Preparation.**  $(\text{OC})_5\text{Mo}(\text{MeDBP})$ , **1**, has been prepared by the reaction of lithium dibenzophospholide with  $\text{Mo}(\text{CO})_6$  in THF, followed by alkylation with methyl iodide.<sup>9</sup> Pale yellow crystals of **1** were isolated from  $\text{CH}_2\text{Cl}_2/\text{methanol}$  at ambient temperature.

\* Address correspondence to these authors. R.E.W.: phone, 902-494-2564; fax, 902-494-1310; e-mail, Roderick.Wasylishen@Dal.Ca. J.H.N.: phone, 702-784-6588; fax, 702-784-6804; e-mail, jhnelson@unr.edu.

<sup>†</sup> Dalhousie University.

<sup>‡</sup> University of Nevada.

<sup>§</sup> McMaster University.

<sup>⊗</sup> Abstract published in *Advance ACS Abstracts*, July 15, 1997.

- (1) Eichele, K.; Wasylishen, R. E.; Kessler, J. M.; Solujić, L.; Nelson, J. H. *Inorg. Chem.* **1996**, *35*, 3904.
- (2) (a) Ramsey, N. F. *Phys. Rev.* **1950**, *78*, 699. (b) Ramsey, N. F. *Phys. Rev.* **1952**, *86*, 243.

- (3) Lindner, E.; Fawzi, R.; Mayer, H. A.; Eichele, K.; Pohmer, K. *Inorg. Chem.* **1991**, *30*, 1102.

- (4) Lindner, E.; Fawzi, R.; Mayer, H. A.; Eichele, K.; Hiller, W. *Organometallics* **1992**, *11*, 1033.

- (5) Kaupp, M. *Chem. Ber.* **1996**, *129*, 535.

- (6) Lumsden, M. D.; Eichele, K.; Wasylishen, R. E.; Cameron, T. S.; Britten, J. F. *J. Am. Chem. Soc.* **1994**, *116*, 11129.

- (7) Lumsden, M. D.; Wasylishen, R. E.; Britten, J. F. *J. Phys. Chem.* **1995**, *99*, 16602.

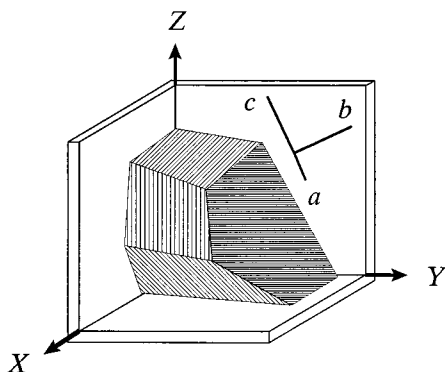
- (8) Naito, A.; Sastry, D. L.; McDowell, C. A. *Chem. Phys. Lett.* **1985**, *115*, 19.

- (9) Maitra, K.; Wilson, W. L.; Jemin, M. M.; Yeung, C.; Rader, W. S.; Redwine, K. D.; Striplin, D. P.; Catalano, V. J.; Nelson, J. H. *Syn. React. Inorg. Met.-Org. Chem.* **1996**, *26*, 967.

**Table 1.** Crystallographic Data for (OC)<sub>5</sub>Mo(MeDBP)

chem formula	C <sub>18</sub> H <sub>11</sub> MoO <sub>5</sub> P
fw	434.18
cryst size (mm)	0.40 × 0.55 × 0.68
cryst system	monoclinic
space group	C2/c
a (Å)	31.113(2)
b (Å)	7.7917(5)
c (Å)	17.9522(12)
β (deg)	122.135(4)
V (Å <sup>3</sup> )	3685.2(4)
Z	8
ρ <sub>calc</sub> (g cm <sup>-3</sup> )	1.565
λ (Å)	Mo Kα, 0.710 73
μ (mm <sup>-1</sup> )	0.822
F(000)	1728
θ range (deg)	2.27–22.49
reflens colld	3022
indepdt reflens	2407
abs corr	ψ scans
params	228
R (R <sub>w</sub> ) <sup>a</sup>	0.0245 (0.0584)
GOF <sup>b</sup>	1.104

<sup>a</sup> Residual index  $R = \sum(|F_o| - |F_c|)/\sum|F_o|$ ; weighted residual  $R_w = [\sum w(F_o^2 - F_c^2)^2/\sum w(F_o^2)]^{0.5}$ . <sup>b</sup> Goodness-of-fit (GOF) =  $S = [\sum w(F_o^2 - F_c^2)^2/(n - p)]^{0.5}$ .

**Figure 1.** Relative orientations of the crystal holder, the NMR cube frame X, Y, Z, and the crystal axes a, b, c of the monoclinic crystal of (OC)<sub>5</sub>Mo(MeDBP).

**X-ray Data Collection and Processing.** A suitable crystal was mounted on a glass fibre and placed on a Siemens P4 diffractometer. Crystal data and details of data collection are given in Table 1. Intensity data were taken in the  $\omega$ -mode. Two check reflections, monitored every 200 reflections, showed random (<2%) variation during the data collection. The data were corrected for Lorentz and polarization effects and for absorption using a semi-empirical model (maximum and minimum transmission factors of 0.6118 and 0.5626). Scattering factors and corrections for anomalous dispersion were taken from a standard source.<sup>10</sup> Calculations were performed on a PC with the Siemens SHELXTL PLUS version 5.1 software package. The structure was solved by the Patterson method. Anisotropic thermal parameters were assigned to all non-hydrogen atoms. Hydrogen atoms were refined at calculated positions with a riding model in which the C–H vector was fixed at 0.96 Å. Final cycles of refinement converged to  $R = 0.0245$  and  $R_w = 0.0584$ , with  $\omega^{-1} = \sigma^2 F + 0.001 F^2$ . The largest peaks in the final difference maps had values of 0.279 and  $-0.223 \text{ e } \text{Å}^{-3}$ .

**NMR Experiments.** A crystal measuring approximately  $2.5 \times 2.5 \times 2.0 \text{ mm}$  was used for the single-crystal NMR experiments. The single crystal was glued onto a hollow three-sided alumina cube measuring 4 mm on each side. The normals to the solid faces of this crystal holder were labeled X, Y, Z in a right-handed fashion. This axis system shall be henceforth referred to as the “cube frame” (Figure 1). The orientation of the crystal axis system with respect to this cube frame was determined using a Siemens P4 four-circle X-ray diffrac-

**Table 2.** Selected Bond Distances (Å) and Bond Angles (deg) for (OC)<sub>5</sub>Mo(MeDBP)

Mo(1)–C(1)	2.052(4)	C(1)–O(1)	1.128(4)
Mo(1)–C(2)	2.032(4)	C(2)–O(2)	1.132(4)
Mo(1)–C(3)	2.003(4)	C(3)–O(3)	1.139(4)
Mo(1)–C(4)	2.038(4)	C(4)–O(4)	1.132(4)
Mo(1)–C(5)	2.035(4)	C(5)–O(5)	1.128(4)
Mo(1)–P(1)	2.4899(9)	P(1)–C(6)	1.832(3)
P(1)–C(7)	1.812(3)	P(1)–C(18)	1.815(3)
C(1)–Mo(1)–C(2)	91.35(13)	C(2)–Mo(1)–P(1)	87.44(10)
C(1)–Mo(1)–C(3)	91.01(14)	C(3)–Mo(1)–C(4)	92.18(14)
C(1)–Mo(1)–C(4)	176.62(13)	C(3)–Mo(1)–C(5)	89.6(2)
C(1)–Mo(1)–C(5)	91.06(14)	C(3)–Mo(1)–P(1)	178.23(10)
C(1)–Mo(1)–P(1)	87.30(10)	C(4)–Mo(1)–C(5)	90.07(14)
C(2)–Mo(1)–C(3)	92.1(2)	C(4)–Mo(1)–P(1)	89.50(9)
C(2)–Mo(1)–C(4)	87.42(14)	C(5)–Mo(1)–P(1)	90.90(11)
C(2)–Mo(1)–C(5)	177.00(14)	Mo(1)–P(1)–C(6)	114.95(12)
Mo(1)–P(1)–C(7)	119.09(11)	Mo(1)–P(1)–C(18)	119.47(11)
C(6)–P(1)–C(7)	104.2(2)	C(6)–P(1)–C(18)	104.9(2)
C(7)–P(1)–C(18)	90.7(2)		

tometer. The Euler angles<sup>11</sup> relating the orthogonalized crystal axis system  $a^*bc$  to the cube frame are  $\alpha = 247.9^\circ$ ,  $\beta = 30.5^\circ$ , and  $\gamma = 120.1^\circ$ . Roughly, the crystal axis  $b$  is contained in the YZ plane of the crystal holder.

Solid-state <sup>31</sup>P NMR experiments were carried out at 81.03 MHz and 161.98 MHz using Bruker MSL-200 and AMX-400 spectrometers ( $B_0 = 4.7$  and 9.4 T, respectively). Single-crystal <sup>31</sup>P NMR spectra were obtained on the AMX-400 spectrometer using an automated single-crystal goniometer probe from Doty Scientific. The cube mount was placed into a hollow cubic receptacle in the goniometer of the probe, with the rotation axis perpendicular to the magnetic field. Spectra were acquired at 9° intervals for rotations about the three orthogonal cube axes X, Y, and Z, respectively. The rotations were controlled by an external stepper motor placed underneath the probe. The <sup>31</sup>P NMR spectra were acquired after cross-polarization (CP) using the Hartmann–Hahn match condition and under high-power proton decoupling, using <sup>1</sup>H pulse widths of 5  $\mu\text{s}$ , contact times of 5 ms, and recycle delays of 20 s. Typically, 40 FIDs were co-added, using a sweep width of 98 kHz and a time domain size of 1 K. Details concerning the analysis of single-crystal NMR experiments performed in our laboratory can be found in the literature.<sup>12</sup>

Phosphorus-31 CP/magic-angle spinning (MAS) NMR spectra were acquired on the MSL-200 using a Bruker double-bearing MAS probe, with 3  $\mu\text{s}$  proton pulse widths and contact times of 5 ms. Chemical shifts were referenced with respect to external 85% aqueous H<sub>3</sub>PO<sub>4</sub> by setting the peak of external NH<sub>4</sub>H<sub>2</sub>PO<sub>4</sub> to 0.8 ppm. Analysis of spectra of static and spinning powder samples was carried out using WSolids and HBA, programs developed in this laboratory.

## Results and Discussion

**Crystal Structure of (OC)<sub>5</sub>Mo(MeDBP).** The crystal structure of (OC)<sub>5</sub>Mo(MeDBP) consists of isolated molecules with no unusual intermolecular contacts. Selected bond lengths and angles are listed in Table 2, and a perspective drawing of one molecule is shown in Figure 2. The Mo–P distance, 2.4899(9) Å, is in the normal range.<sup>13</sup> The bond angles about phosphorus and the structure drawing in Figure 2 indicate the presence of an approximate mirror plane in the molecule, containing Mo(1), P(1), C(6), C(3), and O(3). This observation will become important in assigning the results of the single-crystal <sup>31</sup>P NMR experiment (*vide infra*).

**<sup>31</sup>P NMR Spectra of Powder Samples.** Typical <sup>31</sup>P CP NMR spectra obtained for powder samples of **1** under static

(10) *International Tables for X-Ray Crystallography*; D. Reidel Publishing Co.: Boston, MA, 1992; Vol. C.

(11) Mehring, M. *Principles of High Resolution NMR in Solids*, 2nd revised ed.; Springer-Verlag: Berlin, 1983.

(12) (a) Power, W. P.; Mooibroek, S.; Wasylishen, R. E.; Cameron, T. S. *J. Phys. Chem.* **1994**, *98*, 1552. (b) Eichele, K.; Wasylishen, R. E. *J. Phys. Chem.* **1994**, *98*, 3108. (c) Eichele, K.; Wu, G.; Wasylishen, R. E.; Britten, J. F. *J. Phys. Chem.* **1995**, *99*, 1030.

(13) Davies, M. S.; Aroney, M. J.; Buys, I. E.; Hambley, T. W.; Calvert, J. L. *Inorg. Chem.* **1995**, *34*, 330.

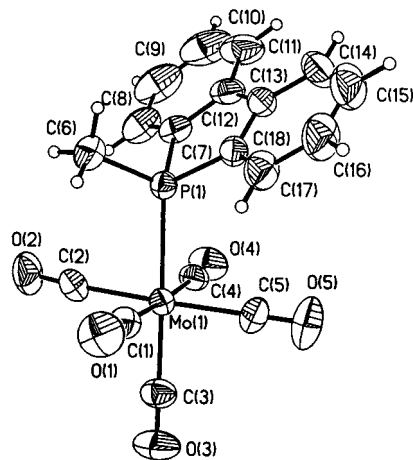


**Figure 2.** Perspective drawing of  $(OC)_5Mo(MeDBP)$  showing the atomic numbering scheme (50% probability ellipsoids). Hydrogen atoms have an arbitrary radius of 0.1 Å.

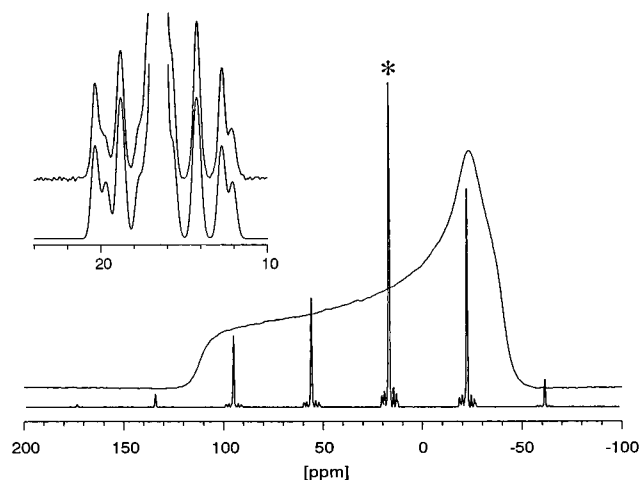


**Figure 3.** Phosphorus-31 CP NMR spectra of powder samples of  $(OC)_5Mo(MeDBP)$  obtained at 4.7 T. The bottom trace shows the MAS spectrum obtained with a spinning rate of 3.20 kHz; the isotropic region is indicated by an asterisk. Satellite peaks due to  $^{95,97}Mo,^{31}P$  spin-spin interactions are clearly visible; the inset shows an expansion of the satellites surrounding the isotropic peak together with a calculated spectrum. The upper trace shows the spectrum of a static powder sample, obtained after 2450 scans.

and MAS conditions are shown in Figure 3. The MAS spectrum shows a single isotropic peak at 16.5 ppm, flanked by spinning sidebands. In addition, satellites due to  $^{95}Mo,^{31}P$  ( $^{95}Mo$ :  $I = 5/2$ ,  $n_a = 15.72\%$ ) and  $^{97}Mo,^{31}P$  ( $^{97}Mo$ :  $I = 5/2$ ,  $n_a = 9.46\%$ ) spin-spin coupling interactions are clearly evident. Although both isotopes of molybdenum have very similar magnetogyric ratios [ $\gamma(^{95}Mo) = -1.7514 \times 10^7 \text{ rad s}^{-1} \text{ T}^{-1}$ ;  $\gamma(^{97}Mo) = -1.7884 \times 10^7 \text{ rad s}^{-1} \text{ T}^{-1}$ ;  $\gamma(^{97}Mo)/\gamma(^{95}Mo) = 1.0211$ ] and therefore very similar indirect Mo,P spin-spin coupling constants,  $J$ , the nuclear quadrupole moments of  $^{95}Mo$  and  $^{97}Mo$  differ in sign and significantly in magnitude [ $Q(^{95}Mo) = -0.022 \times 10^{-28} \text{ m}^2$ ;  $Q(^{97}Mo) = 0.255 \times 10^{-28} \text{ m}^2$ ;  $Q(^{97}Mo)/Q(^{95}Mo) = -11.59$ ].<sup>14</sup> This difference makes it possible to resolve  $^{95}Mo,^{31}P$  and  $^{97}Mo,^{31}P$  spin-spin coupling interactions in the outermost peaks of the multiplet observed in the MAS spectrum.

As demonstrated below, the  $^{95,97}Mo$  quadrupolar coupling constants are sufficiently small that first-order perturbation theory is valid, thus the multiplets in the  $^{31}P$  MAS spectrum

can be analyzed using the following expression:<sup>15</sup>

$$\nu_m = \nu_{iso} - m|J| - \frac{S(S+1) - 3m^2}{S(2S-1)}d \quad (1)$$

Here  $\nu_{iso}$  is the frequency of the uncoupled phosphorus nuclei and  $m$  is the  $z$ -component of the angular momentum of the  $|m\rangle$  state of the quadrupolar nucleus  $S$ , with  $m = S, S-1, \dots, -S$ . The residual dipolar coupling,  $d$ , is given by

$$d = -\frac{3\chi D}{20Z}(3 \cos^2 \beta - 1 + \eta \sin^2 \beta \cos 2\alpha) \quad (2)$$

with the quadrupolar coupling constant  $\chi = e^2 Q q_{zz}/h$  and the asymmetry parameter of the electric field gradient (EFG) tensor  $\eta = (q_{xx} - q_{yy})/q_{zz}$ , with principal components  $|q_{zz}| \geq |q_{yy}| \geq |q_{xx}|$  and the Larmor frequency  $Z = \gamma_S B_0/2\pi$  of the  $S$  nucleus. The dipolar coupling constant,  $D$ , is given by

$$D = \left(\frac{\mu_0}{4\pi}\right) \frac{\gamma_I \gamma_S (\hbar)}{r_{IS}^3} \left(\frac{\hbar}{2\pi}\right) \quad (3)$$

and the azimuthal and polar angles,  $\alpha$  and  $\beta$ , define the orientation of the internuclear vector,  $r_{IS}$ , with respect to the principal axis system of the EFG tensor.

Using this approach, the multiplets arising from  $^{95}Mo$  and  $^{97}Mo$  have been analyzed independently to give  $J$  couplings of 123(2) Hz and  $d$  values of 5(2) Hz ( $^{95}Mo$ ) and  $-48(2)$  Hz ( $^{97}Mo$ ); a calculated spectrum using these parameters is shown in Figure 3. The  $^{31}P$  chemical shift and  $^{95}Mo,^{31}P$  spin-spin coupling constant determined here compare favorably to the values obtained from solution spectra, where  $\delta(^{31}P) = 15.7$  ppm and  $^1J(^{95}Mo,^{31}P)$  has been determined from the  $^{95}Mo$  NMR solution spectrum as 129 Hz.<sup>9</sup> The parameter  $d$  and eq 2 can be used to estimate the  $^{95}Mo$  and  $^{97}Mo$  quadrupolar coupling constants in **1**. Given that the Mo-P distance is 2.4899 Å, the direct dipolar coupling constants calculated using eq 3 are  $D(^{95}Mo,^{31}P) = -206$  Hz and  $D(^{97}Mo,^{31}P) = -211$  Hz. For this complex, which has an approximate  $C_4$  axis (from the perspective of the molybdenum), we assume the electric field gradient tensor at molybdenum to be approximately axially symmetric ( $\eta = 0$ ), with the largest component parallel to the Mo-P bond ( $\beta = 0^\circ$ ). In an applied magnetic field of 4.7 T, the Larmor frequencies of molybdenum are  $Z(^{95}Mo) = 13.09$  MHz and  $Z(^{97}Mo) = 13.36$  MHz. Because the relative error in the value of  $d$  for  $^{97}Mo$  is smaller, this value is used to deduce the following quadrupolar coupling constants:  $\chi(^{95}Mo) = -0.87$  MHz,  $\chi(^{97}Mo) = +10.1$  MHz. In the above analysis, we have assumed that the anisotropy in the indirect spin-spin coupling,  $\Delta J$ , can be neglected. Even for spin systems where  $\Delta J$  is expected to be large,<sup>16</sup> it has been found to be only 70% of the isotropic coupling constant.<sup>6,7</sup> Because  $\Delta J$  modifies the effective dipolar interaction as  $D - \Delta J/3$ , ignoring  $\Delta J$  is expected to cause an error, at most, of 15% in  $d$  and hence  $\chi$ .

In general, the applicability of the first-order perturbation approach should be verified by obtaining spectra at two different applied magnetic fields. If the field dependence of the spectra can be analyzed with the same set of parameters, then the analysis appears to be valid. In the present case, however, the isotopes  $^{95,97}Mo$  with very different nuclear quadrupole moments

(14) (a) Raghavan, P. *At. Data Nucl. Data Tables* **1989**, *42*, 189. (b) Minelli, M.; Enemark, J. H.; Brownlee, R. T. C.; O'Connor, M. J.; Wedd, A. G. *Coord. Chem. Rev.* **1985**, *68*, 169. (c) Kidd, R. G. *J. Magn. Reson.* **1981**, *45*, 88. (d) Brownlee, R. T. C.; Shehan, B. P. *J. Magn. Reson.* **1986**, *66*, 503.

(15) (a) Harris, R. K.; Olivieri, A. C. *Prog. NMR Spectrosc.* **1992**, *24*, 435. (b) Eichele, K.; Wasylishen, R. E.; Corrigan, J. F.; Doherty, S.; Sun, Y.; Carty, A. J. *Inorg. Chem.* **1993**, *32*, 121. (c) Eichele, K.; Wasylishen, R. E. *Inorg. Chem.* **1994**, *33*, 2766. (d) Eichele, K.; Wasylishen, R. E. *Angew. Chem., Int. Ed. Engl.* **1992**, *31*, 1222. (16) (a) Pyykkö, P.; Wiesenfeld, L. *Mol. Phys.* **1981**, *43*, 557. (b) Viste, A.; Hotokka, M.; Laaksonen, L.; Pyykkö, P. *Chem. Phys.* **1982**, *72*, 225.

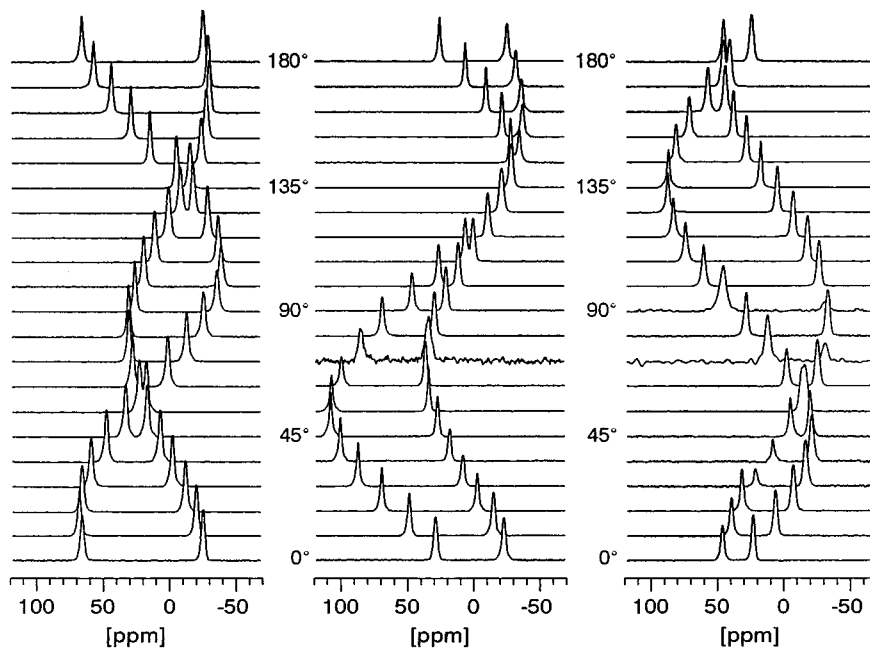


**Figure 4.** Phosphorus-31 CP NMR spectra of a single crystal of  $(OC)_5Mo(MeDBP)$  as a function of crystal orientation in the magnetic field, for rotations about the cube X, Y, and Z axes, from left to right, respectively.

enable one to perform this check at a single applied field. The ratio  $Q(^{97}Mo)/Q(^{95}Mo) = -11.59$  leads to very different values of the parameter  $d$ . In order to obtain a comparable variation in  $d$  by changing the applied magnetic field,  $B_0$ , one would require  $B_0 = 54.47$  T for  $^{97}Mo$  or  $B_0 = 0.41$  T for  $^{95}Mo$ ! The relatively sharp  $^{95}Mo$  peaks observed in solution NMR studies<sup>9</sup> of **1** are clearly a consequence of the relatively small  $^{95}Mo$  nuclear quadrupolar coupling constants.<sup>17</sup>

The intensities of the spinning sidebands in the spectrum of an isolated spin  $1/2$  nucleus are related to the line shape of the static powder spectrum.<sup>18</sup> They can be used to reconstruct the principal components of the chemical shift tensor. From several  $^{31}P$  CP/MAS NMR spectra with spinning rates in the range 1.3–3.2 kHz, the principal components were determined to be  $\delta_{11} = 112.6(8)$  ppm,  $\delta_{22} = -19.2(28)$  ppm, and  $\delta_{33} = -43.9(20)$  ppm. The first derivative of the  $^{31}P$  CP NMR spectrum of a static powder sample was also analyzed to yield the principal components  $\delta_{11} = 112.0(5)$  ppm,  $\delta_{22} = -22.5(5)$  ppm, and  $\delta_{33} = -40.0(5)$  ppm, with an estimated absolute error of 2 ppm. Although the principal components of the phosphorus chemical shift tensor can be obtained from spectra of powder samples with relative ease, there is generally no information available about the orientation of the chemical shift tensor with respect to the molecular frame of reference. Clearly such information is essential in attempting to gain a better understanding of the relationship between molecular structure and chemical shifts. For this reason, we performed a  $^{31}P$  CP NMR experiment on a single crystal of **1**.

**Single-Crystal  $^{31}P$  NMR.**  $^{31}P$  NMR spectra of a single crystal of **1** as a function of crystal orientation in the magnetic field are shown in Figure 4. All phosphorus atoms are crystallographically equivalent; however, crystallographic sites related by a 2-fold axis are magnetically nonequivalent. Therefore, two peaks were observed in general. Peak positions as a function of orientation, so-called rotation patterns, are shown in Figure 5. The peak positions were fit to an equation of the following form:<sup>12,19</sup>

$$\delta_i(\Omega) = A_i + B_i \cos 2\varphi + C_i \sin 2\varphi \quad (4)$$

using a linear least-squares procedure. The resulting nine coefficients from the three rotations  $i = X, Y, Z$ , given in Table 3, were used to construct the chemical shift tensors in the cube frame.<sup>12,19</sup> After diagonalization, the principal components of the CS tensors and their direction cosines in the cube frame were obtained. The crystal symmetry requires that the principal axis systems of the two magnetically distinct chemical shift tensors be related to each other via the 2-fold axis of the monoclinic crystal, corresponding to the crystal  $b$  axis. As an internal check on the agreement between single-crystal NMR and X-ray diffraction, the direction cosines of the  $b$  axis in the cube frame were calculated at this point. From the principal axis systems of the two CS tensors, one obtains  $-0.233(12)$ ,  $0.870(4)$ , and  $0.434(10)$ , while the X-ray diffraction experiment yields  $-0.184$ ,  $0.879$ , and  $0.440$ . The angle between these directions is  $2.9^\circ$ .

After transformation of the CS tensors into the crystal axis system, the magnitudes and orientations of the principal components were averaged, as summarized in Table 4. Because of the existence of magnetically nonequivalent sites, there is a 2-fold ambiguity in assigning the orientation of the CS tensors to an orientation in the molecular frame of reference. In the absence of spin–spin interactions, which may enable the assignment,<sup>6,7,12c,20</sup> one has to rely on possible constraints imposed on the orientation of the principal components by local symmetry.<sup>8,19,21</sup> As outlined in the discussion of the structure of **1**, the molecule possesses a local mirror plane about phosphorus. As a consequence, one principal component of the phosphorus chemical shift tensor must be perpendicular to the local mirror plane, while the two in-plane components experience no further constraints by this symmetry element. However, it is well known that the phosphorus chemical shift of a phosphine ligand generally shifts significantly to higher

(17) Affandi, S.; Nelson, J. H.; Alcock, N. W.; Howarth, O. W.; Alyea, E. C.; Sheldrick, G. M. *Organometallics* **1988**, *7*, 1724.  
 (18) (a) Maricq, M. M.; Waugh, J. S. *J. Chem. Phys.* **1979**, *70*, 3300. (b) Herzfeld, J.; Berger, A. E. *J. Chem. Phys.* **1980**, *73*, 6021.  
 (19) Kennedy, M. A.; Ellis, P. D. *Concepts Magn. Reson.* **1989**, *1*, 109.

(20) Eichele, K.; Wasylshen, R. E.; Corrigan, J. F.; Taylor, N. J.; Carty, A. *J. Am. Chem. Soc.* **1995**, *117*, 6961.  
 (21) (a) Kohler, S. J.; Klein, M. P. *Biochemistry* **1976**, *15*, 967. (b) Kohler, S. J.; Klein, M. P. *J. Am. Chem. Soc.* **1977**, *99*, 8290. (c) Herzfeld, J.; Griffin, R. G.; Haberkorn, R. A. *Biochemistry* **1978**, *17*, 2711. (d) Van Calsteren, M.-R.; Birnbaum, G. I.; Smith, I. C. P. *J. Chem. Phys.* **1987**, *86*, 5405. (e) Hauser, H.; Radloff, C.; Ernst, R. R.; Sundell, S.; Pascher, I. *J. Am. Chem. Soc.* **1988**, *110*, 1054.

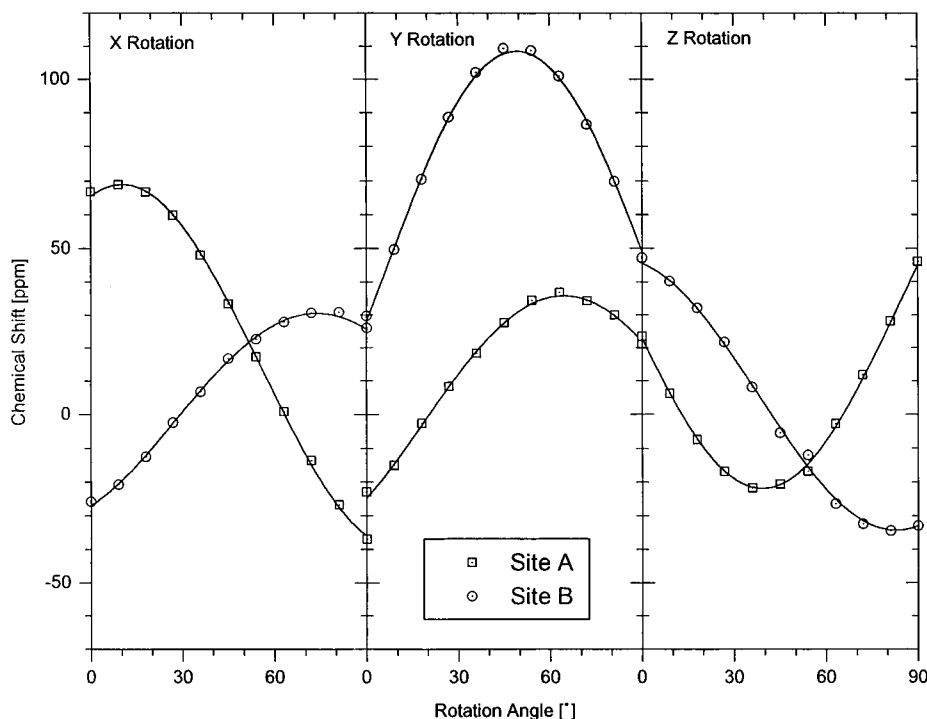


**Figure 5.** Peak positions in the  $^{31}\text{P}$  NMR spectra of a single crystal of  $(\text{OC})_5\text{Mo}(\text{MeDBP})$  as a function of crystal orientation, shown in Figure 4, and least-squares fit.

**Table 3.** Coefficients (in ppm) for the Linear Least-Squares Fit of the  $^{31}\text{P}$  Chemical Shift Interaction of Sites A and B of **1** with Standard Deviations in Units of the Least Significant Digits Given in Parentheses<sup>a</sup>

	site A	site B		site A	site B
$A_X$	14.8(2)	-0.6(1)	$C_Y$	30.5(3)	69.5(4)
$B_X$	37.9(3)	-30.9(2)	$A_Z$	34.0(2)	6.3(3)
$C_X$	38.8(3)	4.1(2)	$B_Z$	-18.7(2)	37.4(4)
$A_Y$	-1.3(2)	38.7(3)	$C_Z$	-52.6(2)	-15.6(4)
$B_Y$	-21.2(3)	-5.5(4)			

<sup>a</sup> Phase angles of  $+12.5^\circ$ ,  $-2^\circ$ , and  $-4^\circ$  for X, Y, and Z rotations, respectively, were used.<sup>19</sup>

**Table 4.** Principal Components (in ppm)<sup>a</sup> of the Averaged  $^{31}\text{P}$  Chemical Shift Tensors of **1** in the Crystal Axis Frame  $a^*bc$ ,<sup>b</sup> with Standard Deviations in Units of the Least Significant Digits Given in Parentheses

	$a^*$		$b$		$c$
$\delta_{11}$	109.1(1)	0.5253(348)	0.3755(494)	-0.7636(4)	
$\delta_{22}$	-22.5(33)	-0.6560(500)	0.7503(411)	-0.0823(237)	
$\delta_{33}$	-40.7(11)	0.5420(269)	0.5442(226)	0.6404(35)	

<sup>a</sup> Relative to external 85% aqueous  $\text{H}_3\text{PO}_4$ , reported on the chemical shift scale:  $\delta_{11} \geq \delta_{22} \geq \delta_{33}$ .<sup>b</sup> Direction cosines are reported such that magnetic site A is assigned to crystallographic site 1. Direction cosines for site B can be generated by applying the symmetry operation  $\bar{x}$ ,  $y$ ,  $\bar{z}$ . The absolute error in the orientations is estimated to be  $5^\circ$ .

frequencies upon coordination to a transition metal.<sup>22</sup> Obviously, the Mo–P bond plays an important role in determining the characteristics of the phosphorus chemical shift tensor. Hence, one would expect one component of the phosphorus shift tensor to be oriented close to the Mo–P bond. The assignment shown in Figure 6 fulfills these expectations quite well, while

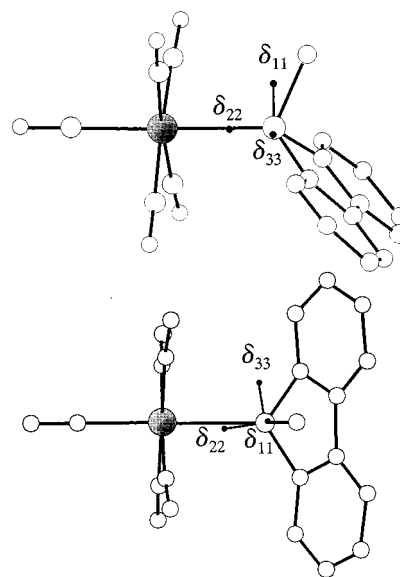


**Figure 6.** Two views of the orientation of the phosphorus chemical shift tensor in the molecular frame of reference of  $(\text{OC})_5\text{Mo}(\text{MeDBP})$ , as determined by single-crystal  $^{31}\text{P}$  NMR. The direction of highest shielding,  $\delta_{33}$ , is perpendicular to the local mirror plane, while  $\delta_{22}$  is close to the Mo–P bond direction. The direction of least shielding,  $\delta_{11}$ , is perpendicular to the Mo–P bond and within the local mirror plane.

the alternative assignment does not show any correlation with the local symmetry or any of the bonds involving phosphorus. For the assignment preferred here, the angles between Mo–P and the principal components are  $87^\circ$  for  $\delta_{11}$ ,  $8^\circ$  for  $\delta_{22}$ , and  $83^\circ$  for  $\delta_{33}$  (but for the alternative assignment the angles are  $55^\circ$  for  $\delta_{11}$ ,  $75^\circ$  for  $\delta_{22}$ , and  $39^\circ$  for  $\delta_{33}$ , with none of the components closer than  $25^\circ$  to the local mirror plane). On the basis of this assignment, the direction of highest shielding,  $\delta_{33}$ , is perpendicular to the local mirror plane. The angle between  $\delta_{22}$  and Mo–P is  $8^\circ$ , and that between  $\delta_{11}$  and Mo–P is  $87^\circ$ . It is remarkable that both the direction of highest and that of least shielding are perpendicular to the Mo–P bond! This strongly suggests that the electronic environment about phosphorus

(22) (a) Meriwether, L. S.; Leto, J. R. *J. Am. Chem. Soc.* **1961**, *83*, 3192. (b) Grim, S. O.; Keiter, R. L. *Inorg. Chim. Acta* **1970**, *4*, 56. (c) Mann, B. E.; Masters, C.; Shaw, B. L.; Slade, R. M.; Stainbank, R. E. *Inorg. Nucl. Chem. Lett.* **1971**, *7*, 881. (d) Verstuyft, A. W.; Nelson, J. H.; Cary, L. W. *Inorg. Nucl. Chem. Lett.* **1976**, *12*, 53. (e) Nelson, J. H.; Mathey, F. In *Phosphorus-31 NMR Spectroscopy in Stereochemical Analysis: Organic Compounds and Metal Complexes*; Verkade, J. G., Quin, L. D., Eds.; Methods in Stereochemical Analysis 8; VCH Publishers, Inc.: Deerfield Beach, FL, 1987; pp 665–694.

**Table 5.** Phosphorus-31 Chemical Shift Tensors<sup>a</sup> of Tertiary Phosphine Molybdenum(0) and Molybdenum(II) Complexes<sup>b</sup> Reported in the Literature

	$\delta_{\text{iso}}$	$\delta_{11}$	$\delta_{22}$	$\delta_{33}$	$\Omega^c$	$\kappa^d$	ref
(OC) <sub>5</sub> Mo(MeDBP), <b>1</b>	16.5	112	-23	-40	152	-0.776	
(OC) <sub>5</sub> Mo(PhDBP)	28.0	104	24	-44	148	-0.081	1
<i>cis</i> -(OC) <sub>4</sub> Mo(PhDBP) <sub>2</sub>	33.3	89	50	-40	129	0.395	1
	24.5	102	12	-40	142	-0.268	
<i>cis</i> -(OC) <sub>4</sub> Mo( $\eta^2$ -dppm)	2	122	-42	-74	196	-0.674	4
	-4	88	-31	-69	157	-0.516	
<i>cis</i> -(OC) <sub>4</sub> Mo( $\eta^2$ -dppe)	58	162	76	-65	227	0.242	4
	53	155	61	-57	212	0.113	
<i>cis</i> -(OC) <sub>4</sub> Mo( $\eta^2$ -dppp)	14	78	-7	-31	109	-0.560	4
<i>cis</i> -(OC) <sub>4</sub> Mo( $\eta^2$ -dppb)	32	71	71	-46	117	1.000	4
	31	70	70	-47	117	1.000	
	21	86	21	-43	129	-0.008	
	20	85	20	-44	129	-0.008	
<i>cis</i> -(OC) <sub>4</sub> Mo( $\eta^2$ -dpppe)	29	100	21	-35	135	-0.170	4
	27	104	15	-39	143	-0.256	
	25	91	24	-40	131	-0.023	
<i>fac</i> -(OC) <sub>3</sub> Mo( $\eta^3$ -etp)	85	193	135	-73	266	0.564	4
	60	164	82	-65	229	0.284	
	52	156	64	-65	221	0.167	
<i>cis</i> -( $\eta^5$ -C <sub>5</sub> H <sub>5</sub> )(OC) <sub>2</sub> -Mo[ $\eta^2$ -PPH <sub>2</sub> (CH <sub>2</sub> ) <sub>3</sub> ]	100	209	143	-50	259	0.490	3
<i>cis</i> -( $\eta^5$ -C <sub>5</sub> H <sub>5</sub> )(OC) <sub>2</sub> -Mo[ $\eta^2$ -PPH <sub>2</sub> (CH <sub>2</sub> ) <sub>4</sub> ]	51	154	34	-34	188	-0.277	3

<sup>a</sup> Relative to external 85% aqueous H<sub>3</sub>PO<sub>4</sub>, reported on the chemical shift scale:  $\delta_{11} \geq \delta_{22} \geq \delta_{33}$ . <sup>b</sup> dppm = bis(diphenylphosphino)methane; dppe = 1,2-bis(diphenylphosphino)ethane; dppp = 1,3-bis(diphenylphosphino)propane; dppb = 1,4-bis(diphenylphosphino)butane; dppe = 1,5-bis(diphenylphosphino)pentane; etp = bis[2-(diphenylphosphino)ethyl]phenylphosphine, (Ph<sub>2</sub>PCH<sub>2</sub>CH<sub>2</sub>)<sub>2</sub>PPh. <sup>c</sup> Span ( $\Omega$ ) =  $\delta_{11} - \delta_{33}$ . <sup>d</sup> Skew ( $\kappa$ ) =  $3(\delta_{22} - \delta_{\text{iso}})/\Omega$ .

deviates considerably from axial symmetry. Sometimes it is tempting to assign the orientation of a chemical shift tensor in the molecular frame on the basis of the appearance of the static spectrum. In the present case, the powder spectrum shown in Figure 3 might lead one to believe that  $\delta_{11}$  is directed along the Mo–P bond and that the environment about phosphorus is almost axially symmetric, in contrast to our experimental findings here. Actually, the notion of axial symmetry is quite prevalent in the literature, in combination with the reasoning that the direction of highest shielding should be along the metal–phosphorus bond, because of the high electron density arising from the metal in this direction. In Table 5, we have collected the phosphorus chemical shift tensors reported so far for complexes of molybdenum. If the supposition just mentioned were true, the skew  $\kappa$  of the chemical shift tensor should be approximately +1. As evident, this is rarely the case, and, in fact, often a skew of the opposite sign is observed! This is, in part, a consequence of the nature of the data available. In several of the complexes compiled in Table 5, phosphorus is part of a small ring, where a small endocyclic M–P–C angle leads to a considerable deviation of the M–PC<sub>3</sub> fragment from idealized C<sub>3</sub> symmetry. Even in the case of Wilkinson's catalyst<sup>8</sup> and other complexes of the triphenylphosphine ligand,<sup>23</sup> the <sup>31</sup>P chemical shift tensors are clearly nonaxially symmetric. It appears that the local C<sub>3</sub> symmetry of the free tertiary phosphine cannot be preserved in octahedral or square planar metal complexes, resulting in a local mirror plane as the highest element of local symmetry. There are only rare examples where an actual C<sub>3</sub> axis of the complex enforces axially symmetric phosphorus chemical shift tensors.<sup>24</sup>

It is instructive to compare the <sup>31</sup>P chemical shift tensors of (OC)<sub>5</sub>Mo(MeDBP) and (OC)<sub>5</sub>Mo(PhDBP), the first two entries of Table 5. From an electronic point of view the structure at

the phosphorus is more symmetrical in the 5-phenyl derivative. One can think of the PhDBP ligand as consisting of three phenyl rings, while the MeDBP ligand consists of a methyl group and two phenyl rings. Indeed, there is ample evidence in the literature that the PhDBP is analogous to the triphenylphosphine ligand. For example, in our previous <sup>31</sup>P NMR study of solid PhDBP and its derivatives we noticed that the phosphorus chemical shift tensors of the PPh<sub>3</sub> and PhDBP derivatives are very similar, except for a slightly greater asymmetry in the latter class of compounds.<sup>1</sup> Basically, solid PPh<sub>3</sub> and PhDBP differ in their values for  $\delta_{22}$ : 9 and -19 to -22 ppm, respectively. From Table 5, it is clear that on replacing the 5-methyl group by a phenyl group, the isotropic <sup>31</sup>P chemical shift increases by approximately 12 ppm. This high-frequency shift is typical of that observed for other phosphines when methyl is replaced by phenyl. The empirical shift contribution of a phenyl group relative to a methyl group is generally taken to be 18 ppm.<sup>25</sup>

More interesting is the behavior of the principal components of the <sup>31</sup>P chemical shift tensors in (OC)<sub>5</sub>Mo(MeDBP) and (OC)<sub>5</sub>Mo(PhDBP). First, the principal component approximately along the P–C bond axis of the Me or Ph group,  $\delta_{11}$ , shifts to lower frequency (by -8 ppm) on replacing methyl by phenyl. The component approximately along the Mo–P bond axis changes from -23 ppm in the MeDBP complex to -44 ppm in the PhDBP complex, a change of -21 ppm. The remaining principal component, which is approximately perpendicular to the P–C(Me,Ph) bond axis and the Mo–P bond axis, changes from -40 to 24 ppm, a total change of 64 ppm. Clearly, it is this component of the phosphorus shift tensor that is responsible for the observed high-frequency isotropic shift on going from (OC)<sub>5</sub>Mo(MeDBP) to (OC)<sub>5</sub>Mo(PhDBP).

From this study, it is apparent that rather subtle variations in the electronic structure and local symmetry can dictate the orientation of phosphorus chemical shift tensors in transition metal complexes. Furthermore, this work emphasizes the danger of speculating about the shielding tensor orientation on the basis of the observed chemical shift powder pattern in a single compound. Clearly, much more shielding tensor data—principal components and orientations—together with high-level theoretical calculations will be required to better understand phosphorus shielding in transition metal complexes. In this sense, the present study represents a preliminary step in solving a complicated problem. It is hoped this research will stimulate others to recognize the advantages of single-crystal NMR spectroscopy in characterizing NMR chemical shift tensors.

**Acknowledgment.** We wish to thank the Natural Sciences and Engineering Research Council of Canada (NSERC) for financial assistance in the form of equipment and operating grants (R.E.W.). J.H.N. thanks the donors of the Petroleum Research Fund, administered by the American Chemical Society, for financial support. All solid-state spectra were recorded at the Atlantic Region Magnetic Resonance Centre, which is also supported by the NSERC. R.E.W. acknowledges the Canada Council for a Killam Research Fellowship.

**Supporting Information Available:** An X-ray crystallographic file in CIF format for the complex (5-methyldibenzophosphole)penta-carbonylmolybdenum(0) is available on the Internet only. Access information is given on any current masthead page.

IC970260Q

(23) Huang, Y.; Uhm, H. L.; Gilson, D. F. R.; Butler, I. S. *Inorg. Chem.* **1997**, *36*, 435.  
 (24) Wasylishen, R. E.; Wright, K. C.; Eichele, K.; Cameron, T. S. *Inorg. Chem.* **1994**, *33*, 407.

(25) (a) Grim, S. O.; McFarlane, W.; Davidoff, E. F. *J. Org. Chem.* **1967**, *32*, 781. (b) Grim, S. O.; Davidoff, E. F.; Marks, T. J. *Z. Naturforsch.* **1971**, *26b*, 184. (c) Dixon, K. R. In *Multinuclear NMR*; Mason, J., Ed.; Plenum Press: New York, 1987; p 369.